Inorg. Chem. **2004**, *43*, 5128–5133

Inorganic Chemistry
Article

Mixed Valence Aspects of Diruthenium Complexes $[\{(L)ClRu\}_2(\mu\text{-tppz})]^{n+}$ Incorporating 2-(2-Pyridyl)azoles (L) as Ancillary Functions and 2,3,5,6-Tetrakis(2-pyridyl)pyrazine (Tppz) as Bis-Tridentate Bridging Ligand

Nripen Chanda,[†] Biprajit Sarkar,[‡] Sanjib Kar,[†] Jan Fiedler,[§] Wolfgang Kaim,*,[‡] and
Goutam Kumar Lahiri*,[†]

Department of Chemistry, Indian Institute of Technology-Bombay, Powai, Mumbai-400076, India,
Institut fuer Anorganische Chemie, Universitaet Stuttgart, Pfaffenwaldring 55,
D-70550, Stuttgart, Germany, and J. Heyrovsky Institute of Physical Chemistry,
Academy of Science of the Czech Republic, Dolejskova 3, CZ-18223 Prague, Czech Republic

Received March 24, 2004

Tppz [2,3,5,6-tetrakis(2-pyridyl)pyrazine]-bridged complexes $[\{(L)ClRu\}_2(\mu\text{-tppz})]^{n+}$ with structurally similar but electronically different ancillary ligands, 2-(2-pyridyl)azoles (L), were synthesized as diruthenium(II) species. Cyclic voltammetry, EPR of paramagnetic states, and UV–vis–NIR spectroelectrochemistry show that the first two reduction processes occur at the tppz bridge and that oxidation involves mainly the metal centers. The mixed valent intermediates from one-electron oxidation exhibit moderate comproportionation constants $10^4 < K_c < 10^5$ but appear to be valence-averaged according to the Hush criterion. Redox potentials, EPR, and UV–vis–NIR results show the effect of increasing donor strength of the ancillary ligands along the sequence $L^1 < L^2 < L^4 \ll L^3$, L^1 = 2-(2-pyridyl)benzoxazole, L^2 = 2-(2-pyridyl)benzthiazole, L^3 = 2-(2-pyridyl)benzimidazolate, L^4 = 1-methyl-2-(2-pyridyl)-1*H*-benzimidazole. Whereas the mixed valent complexes with L^1 and L^2 remain EPR silent at 4 K, the analogues with L^4 and L^3 exhibit typical ruthenium(III) EPR signals, albeit with some noticeable ligand contribution in the case of the L^3-containing complex. Intervalence charge transfer (IVCT) bands were found in the visible spectrum for the complex with L^3 but in the near-infrared range (at ca. 1500 nm) for the other systems.

Introduction

The discovery of pyrazine-mediated intermetallic electronic coupling in the diruthenium(II,III) Creutz–Taube ion[1] has initiated continuous efforts in designing more elaborate classes of diruthenium complexes[2] incorporating polyazine-based bridging heterocycles such as 2,2′-bipyrimidine,[3] 2,3-bis(2-pyridyl)pyrazine,[4] tetrapyrido[2,3-*a*:3′,2′-*c*:2″,3″-*h*:3″,2″-*j*] phenazine,[5] or 2,3,5,6-tetrakis(2-pyridyl)pyrazine (tppz).[6] In this context, the efficacy of the nonplanar bis-tridentate tppz bridging moiety has been scrutinized recently in polynuclear ruthenium complexes in combination with a wide variety of ancillary ligands.[6] This has led to a considerable variation of the comproportionation constants, K_c's, in the mixed valent states of the complexes $(L')Ru^{II}(\mu\text{-tppz})Ru^{III}(L')$, depending on the electronic nature of L′: $L' = (NH_3)_3$, $K_c = 4.4 \times 10^8$;[6a] 2,2′-dipyridylamine and Cl, $K_c = 2.7 \times 10^6$;[6b] 4′-vinyl- 2,2′:6′,2″-terpyridine (V-trpy),

---

* Authors to whom correspondence should be addressed. E-mail: lahiri@chem.iitb.ac.in (G.K.L.); kaim@iac.uni-stuttgart.de (W.K.).

[†] Indian Institute of Technology-Bombay.

[‡] Universitaet Stuttgart.

[§] Academy of Science of the Czech Republic.

(1) (a) Creutz, C.; Taube, H. *J. Am. Chem. Soc*. **1969**, *91*, 3988. (b) Creutz, C.; Taube, H. *J. Am. Chem. Soc*. **1973**, *95*, 1086. (c) Fuerholz, U.; Joss, S.; Buergi, H. B.; Ludi, A. *Inorg. Chem*. **1985**, *24*, 943. (d) Creutz, C. *Prog. Inorg. Chem*. **1983**, *20*, 1.

(2) Kaim, W.; Klein, A.; Glöckle, M. *Acc. Chem. Res*. **2000**, *33*, 755.

(3) (a) Petersen, J. D.; Murphy, W. R., Jr.; Sahai, R.; Brewer, K.; Ruminski, R. R. *Coord. Chem. Rev*. **1985**, *64*, 261. (b) Dose, E. V.; Wilson, L. J. *Inorg. Chem*. **1978**, *17*, 2660. (c) Hunziker, M.; Ludi, A. *J. Am. Chem. Soc*. **1977**, *99*, 7370. (d) Ruminski, R. R.; Petersen, J. D. *Inorg. Chem*. **1982**, *21*, 3706.

(4) (a) Braunstein, C. H.; Baker, A. D.; Strekas, T. C.; Gafney, H. D. *Inorg. Chem*. **1984**, *23*, 857. (b) Ruminski, R. R.; Cockroft, T.; Shoup, M. *Inorg. Chem*. **1988**, *27*, 4026. (c) Balzani, V.; Juris, A.; Venturi, M.; Campagna, S.; Serroni, S. *Chem. Rev*. **1996**, *96*, 759. (d) Serroni, S.; Campagna, S.; Denti, G.; Keyes, T. E.; Vos, J. G. *Inorg. Chem*. **1996**, *35*, 4513.

(5) (a) Gourdon, A.; Launay, J.-P. *Inorg. Chem*. **1998**, *37*, 5336. (b) Bonhote, P.; Lecas, A.; Amouyal, E. *Chem. Commun*. **1998**, 885.

10.1021/ic049605c CCC: $27.50

Scheme 1

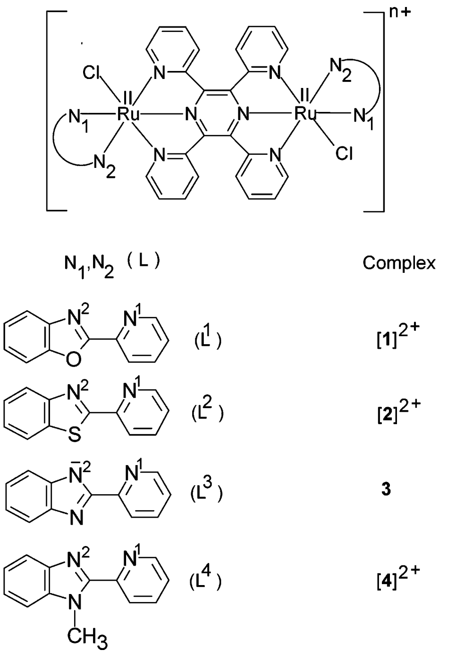

$K_c = 1.3 \times 10^6$;[6c] 2,2′:6′,2″-terpyridine (trpy), $K_c = 1.7 \times 10^5$;[6c] 4′-tolyl- 2,2′:6′,2″-terpyridine (ttrpy), $K_c = 1.3 \times 10^6$;[6d] 2,2′-bipyridine (bpy) and Cl, $K_c = 8.2 \times 10^4$;[6e] 2-phenylazopyridine and Cl, $K_c = 7.9 \times 10^3$.[6f] The distinct role of ancillary functionalities for the $\mathrm{Ru^{II}}(\mu\text{-tppz})\mathrm{Ru^{III}}$ core in terms of the extent of electronic coupling in the mixed valent $\mathrm{Ru^{II}Ru^{III}}$ state has initiated the present program of selective introduction of pyridyl-based heterocycles, viz., 2-(2-pyridyl)azoles, as ancillary ligands.

The work reported in this paper describes the synthesis and characterization of new tppz-bridged diruthenium complexes $[\{(\mathrm{L^{1-4}})\mathrm{ClRu^{II}}\}_2(\mu\text{-tppz})]^{n+}$ ($[\mathbf{1}]^{n+}-[\mathbf{4}]^{n+}$, Scheme 1), involving α-diimine-based 2-(2-pyridyl)azoles as ancillary functionalities: L^1 = 2-(2-pyridyl)benzoxazole, L^2 = 2-(2-pyridyl)benzthiazole, L^3 = 2-(2-pyridyl)benzimidazolate, L^4 = 1-methyl-2-(2-pyridyl)-1*H*-benzimidazole. The mixed valence properties of the complexes have been studied by detailed spectroelectrochemical and EPR investigations. It may be noted that the coordination aspects of 2-(2-pyridyl)azole ligands ($\mathrm{L^1-L^4}$), in general and with the ruthenium ion in particular, have been confined to a limited number of studies.[7]

Results and Discussion

Synthesis and Characterization of the Complexes. Complexes $[(\mathrm{L^{1-4}})\mathrm{ClRu^{II}}(\mu\text{-tppz})\mathrm{Ru^{II}Cl}(\mathrm{L^{1-4}})]^{n+}$ ($[\mathbf{1}]^{n+}-[\mathbf{4}]^{n+}$) were synthesized via reactions of the appropriate 2-(2-pyridyl)azoles ($\mathrm{L^1-L^4}$) with the diruthenium(III) precursor complex $\{\mathrm{Cl_3Ru^{III}}\}_2(\mu\text{-tppz})$ (Scheme 1).

Complexes $[\mathbf{1}]^{2+}$, $[\mathbf{2}]^{2+}$, and $[\mathbf{4}]^{2+}$ are 1:2 electrolytes in acetonitrile (see the Experimental Section), whereas complex **3**, incorporating the ancillary ligand L^3 = 2-(2-pyridyl)-benzimidazolate, is found to be nonconducting. Thus, the anionic nitrogen center (N^2) of the benzimidazolate ring of L^3 is selectively coordinated in **3**, while in other complexes,[7a,g,i,l] the neutral form of L^3, i.e., with proton attached to the noncoordinated imidazole nitrogen, was found to be coordinated preferentially. The presence of a basic reaction medium including $\mathrm{NEt_3}$ may have facilitated the dissociation of the NH proton of L^3 in **3**; this NH proton was found to be absent in the ^{1}H NMR and IR spectra of the complex. However, in $[\mathbf{1}]^{2+}$, $[\mathbf{2}]^{2+}$, and $[\mathbf{4}]^{2+}$, the neutral nitrogen centers of the benzoxazole, benzthiazole, and 1-methylbenzimidazole groups are coordinated in the usual manner.[7] The cationic complexes $[\mathbf{1}]^{2+}$, $[\mathbf{2}]^{2+}$, and $[\mathbf{4}]^{2+}$ have been isolated as perchlorates.

The complexes exhibited satisfactory microanalytical data (see the Experimental Section). Intense perchlorate vibrational bands are observed near 1100 and 640 $\mathrm{cm^{-1}}$. The formation of the complexes was confirmed by their electrospray mass spectra (Supporting Information Figures S1−S4) which displayed molecular ion peaks at 1152.77, 1185.89, 1051.0, and 1179.98, corresponding to $\{[\mathbf{1}](\mathrm{ClO_4})\}^+$ (calculated molecular mass 1153.34), $\{[\mathbf{2}](\mathrm{ClO_4})\}^+$ (calcd 1185.47), $\{\mathbf{3}\}^+$ (calcd 1050.03), and $\{[\mathbf{4}](\mathrm{ClO_4})\}^+$ (calcd 1179.43), respectively.

The unsymmetrical nature of L (N^1 and N^2 as coordinated donor atoms) leads to the possibility of six geometrical isomers (Scheme 2), three each for the *trans* and *cis* configurations, with respect to the mutual orientation of the two chloride ligands (**A**−**F**). Because the isolated green complexes are isomerically pure and exhibit similar spectral profiles (see text to follow), it may be considered that all four complexes were formed as the same kind of isomers.

---

(6) (a) Ruminski, R.; Kiplinger, J.; Cockroft, T.; Chase, C. *Inorg. Chem.* **1989**, *28*, 370. (b) Chanda, N.; Sarkar, B.; Fiedler, J.; Kaim, W.; Lahiri, G. K. *Dalton Trans.* **2003**, 3550. (c) Arana, C. R.; Abruna, H. D. *Inorg. Chem.* **1993**, *32*, 194. (d) Collin, J. P.; Laine, P.; Launay, J. P.; Sauvage, J. P.; Sour, A. *J. Chem. Soc., Chem. Commun.* **1993**, 434. (e) Hartshorn, V.; Daire, N.; Tondreau, V.; Loeb, B.; Meyer, T. J.; White, P. S. *Inorg. Chem.* **1999**, *38*, 3200. (f) Chanda, N.; Laye, R. H.; Chakraborty, S.; Paul, R. L.; Jeffery, J. C.; Ward, M. D.; Lahiri, G. K. *J. Chem. Soc., Dalton Trans.* **2002**, 3496. (g) Thummel, R. P.; Chirayil, S. *Inorg. Chim. Acta* **1988**, *154*, 77. (h) Vogler, L. M.; Scott, B.; Brewer, K. J. *Inorg. Chem.* **1993**, *32*, 898. (i) Lee, J.-D.; Vrana, L. M.; Bullock, E. R.; Brewer, K. J. *Inorg. Chem.* **1998**, *37*, 3575. (j) Akasheh, T. S.; Marji, D.; Al Ahmed, Z. M. *Inorg. Chim. Acta* **1988**, *141*, 125. (k) Vogler, L. M.; Brewer, K. J. *Inorg. Chem.* **1996**, *35*, 818. (l) Dattelbaum, D. M.; Hartshorn, C. M.; Meyer, T. J. *J. Am. Chem. Soc.* **2002**, *124*, 4938. (m) Demandis, K. D.; Hartshorn, C. M.; Meyer, T. J. *Chem. Rev.* **2001**, *101*, 2655. (n) Carranza, J.; Brennan, C.; Sletten, J.; Clemente-Juan, J. M.; Lloret, F.; Julve, M. *Inorg. Chem.* **2003**, *42*, 8716.

(7) Selected references: (a) Haga, M.-A.; Tsunemitsu, A. *Inorg. Chim. Acta* **1989**, *164*, 137. (b) Sheng-Zhi, H.; Dashuang, S.; Taishan, H.; Jiazhu, W.; Zexing, H.; Jinlong, Y.; Chenghui, X. *Inorg. Chim. Acta* **1990**, *173*, 1. (c) Mansingh, P. S.; Mohanty, R. R.; Jena, S.; Dash, K. C. *Indian J. Chem., Sect. A* **1996**, *35A*, 479. (d) Thakur, P.; Chakravortty, V.; Dash, K. C. *Indian J. Chem., Sect. A* **1999**, *38A*, 1223. (e) Maji, M.; Sengupta, P.; Chattopadhyay, S. K.; Mostafa, G.; Schwalbe, C. H.; Ghosh, S. *J. Coord. Chem.* **2001**, *54*, 13. (f) Chen, X.; Femia, F. J.; Babich, J. W.; Zubieta, J. *Inorg. Chim. Acta* **2001**, *314*, 91. (g) Park, S. J.; Kim, D. H.; Kim, D. H.; Park, H. J.; Lee, D. N.; Kim, B. H.; Lee, W.-Y. *Anal. Sci.* **2001**, *17*, a93. (h) Gangopadhyay, J.; Sengupta, S.; Bhattacharyya, S.; Chakraborty, I.; Chakravorty, A. *Inorg. Chem.* **2002**, *41*, 2616. (i) Yi, H.; Crayston, J. A.; Irvine, J. T. S. *Dalton Trans.* **2003**, 685. (j) Panda, B. K.; Ghosh, K.; Chattopadhyay, S.; Chakravorty, A. *J. Organomet. Chem.* **2003**, *674*, 107. (k) Sengupta, S.; Gangopadhyay, J.; Chakravorty, A. *Dalton Trans.* **2003**, 4635. (l) Kim, B. H.; Lee, D. N.; Park, H. J.; Min, J. H.; Jun, Y. M.; Park, S. J.; Lee, W.-Y. *Talanta* **2004**, *62*, 595. (m) Reinhardt, R.; Kaim, W. *Z. Anorg. Allg. Chem.* **1993**, *619*, 1998. (n) Haga, M.; Ishizuya, M.; Kanesugi, T.; Sakiyama, D.; Fees, J.; Kaim, W. *Indian J. Chem., Sect. A* **2003**, *42A*, 2290.

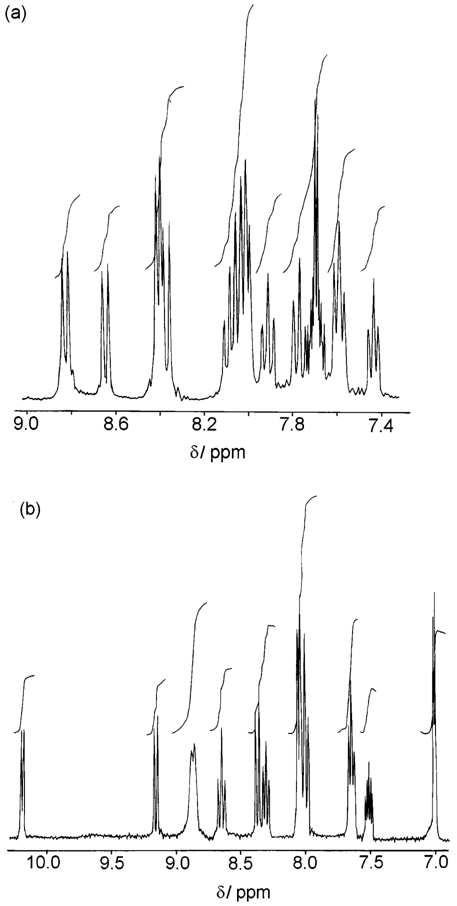

Figure 1. ^{1}H NMR spectra of (a) [{(L^1)ClRu^{II}}$_2$(μ-tppz)](ClO$_4$)$_2$, [**1**](ClO$_4$)$_2$, and (b) [{(L^2)ClRu^{II}}$_2$(μ-tppz)](ClO$_4$)$_2$, [**2**](ClO$_4$)$_2$, in (CD$_3$)$_2$SO.

Scheme 2

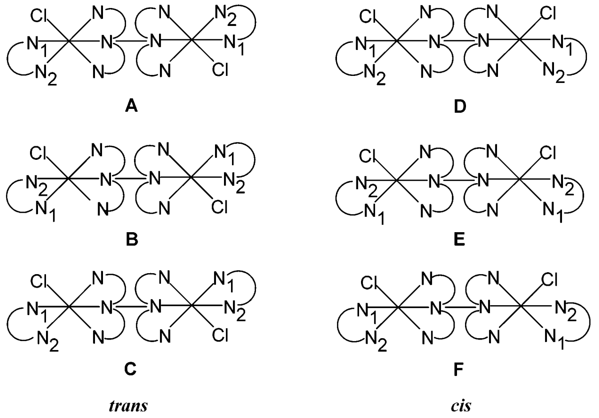

The specific observation of one Ru−Cl band near 300 cm^{-1} and the partial overlap of 16 distinct aromatic proton NMR signals corresponding to one-half of the molecule (Figure 1, 8 from L and 8 from the two inequivalent pyridyl rings of the bridging tppz unit in each of the complexes) are consistent with the symmetrical structures **A**, **B**, **D**, or **E**. In analogous tppz-bridged diruthenium complexes containing 2-phenylazopyridine[6f] or 2-dipyridylamine[6b] ancillary ligands, structure **A** was reported to be the exclusive product, and in the case of L = 2,2′-bipyridine, complex **A** was obtained as a major product.[6e] Therefore, in corroboration with earlier results, we assume that the same *trans* form (**A**) is also the preferred isomer of the present set of complexes.

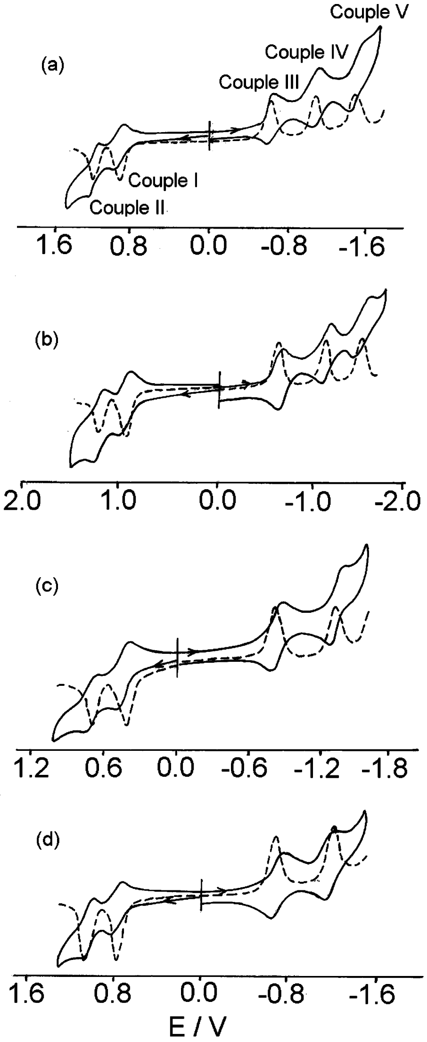

Figure 2. Cyclic voltammograms and differential pulse voltammograms of (a) [{(L^1)ClRu^{II}}$_2$(μ-tppz)](ClO$_4$)$_2$, [**1**](ClO$_4$)$_2$, (b) [{(L^2)ClRu^{II}}$_2$(μ-tppz)](ClO$_4$)$_2$, [**2**](ClO$_4$)$_2$, (c) [{(L^3)ClRu^{II}}$_2$(μ-tppz)], **3**, and (d) [{(L^4)ClRu^{II}}$_2$-(μ-tppz)](ClO$_4$)$_2$, [**4**](ClO$_4$)$_2$ in CH$_3$CN/0.1 M Et$_4$NClO$_4$.

Electrochemistry. Each of the complexes [**1**]$^{2+}$, [**2**]$^{2+}$, **3**, and [**4**]$^{2+}$ exhibits what appears to be two successive quasireversible Ru^{III}/Ru^{II} couples (couple I and couple II) in the potential range between 0.4 and 1.23 V versus SCE, depending on the nature of the ancillary ligands (Figure 2, Table 1). The stability of the Ru^{II} state follows the order [**2**]$^{2+}$ > [**1**]$^{2+}$ > [**4**]$^{2+}$ > **3**. The presence of the anionic form of L^3 in **3** reduces the Ru^{III}/Ru^{II} potential by 350 mV with respect to the analogous N-methylated derivative ([**4**]$^{2+}$), destabilizing the Ru^{II} state. Although a substantial decrease in the potentials of the Ru^{III}/Ru^{II} couples has thus been observed along the series [**2**]$^{2+} \rightarrow$ [**1**]$^{2+} \rightarrow$ [**4**]$^{2+} \rightarrow$ **3**, the potential separation between the successive Ru^{III}/Ru^{II} couples remains rather constant among the complexes (Table 1). Analogous tppz-bridged diruthenium complexes containing other types of ancillary ligands such as 2-phenylazopyridine,[6f] 2,2′-bipyridine,[6e] or 2,2′-dipyridylamine[6b] displayed the first Ru^{III}/Ru^{II} couples at 1.28, 0.96, and 0.68 V versus SCE, respectively. Therefore, the effect of the ancillary ligands on the stability of the Ru^{II} state follows the ligand order 2-phenylazopyridine > 2,2′-bipyridine > L^2 > L^1 > L^4 >

Table 1. Electrochemical Data at 298 K[a]

	$E°_{298}$/V (ΔE_p/mV)								
	Ru(III)−Ru(II) couple		ligand based reductions						
compd	couple I	couple II	couple III	couple IV	couple V	ancillary ligand	E_{pa}[b]	ΔE/V couple II−couple I	K_c[c]
$[\mathbf{1}]^{2+}$	0.92(60)	1.19(77)	−0.63(60)	−1.10(60)	−1.51(110)	L^1	−1.01	0.270	3.8×10^4
$[\mathbf{2}]^{2+}$	0.95(60)	1.23(85)	−0.59(95)	−1.10(60)	−1.48(140)	L^2	−1.16	0.280	5.6×10^4
3	0.43(90)	0.69(85)	−0.84(70)	−1.37(97)		L^3	−1.24	0.260	2.6×10^4
$[\mathbf{4}]^{2+}$	0.78(90)	1.04(90)	−0.71(80)	−1.19(65)		L^4	−1.27	0.260	2.6×10^4

[a] Solvent, acetonitrile; supporting electrolyte, $[NEt_4][ClO_4]$; reference electrode, SCE; solute concentration, 10^{-3} M; working electrode, platinum wire; scan rate, 50 mV s^{-1}; $E°_{298} = 0.5(E_{pa} + E_{pc})$, where E_{pa} and E_{pc} are anodic and cathodic peak potentials, respectively. [b] E_{pa} is considered due to irreversible process. [c] Calculated by using the equation $RT \ln K_c = nF(\Delta E)$.

2,2′-dipyridylamine ≫ L^3. The 260−280 mV potential separation between the stepwise Ru^{III}/Ru^{II} couples in the present set of complexes leads to comproportionation constants (K_c's) in the range between 2.6×10^4 and 5.6×10^4 [calculated by using the equation $RT \ln K_c = nF(\Delta E)$[8]] (Table 1). This indicates moderate intermetallic electrochemical coupling across the tppz bridging ligand in the mixed valent states of the complexes. The corresponding 2,2′-dipyridylamine,[6b] 2,2′-bipyridine,[6e] and 2-phenylazopyridine[6f] derivatives exhibited K_c values of 2.7×10^6, 8.2×10^4, and 7.9×10^3, respectively. The systematic decrease of K_c with the increase in π acidity of the ancillary ligands illustrates a less efficient electron-transfer-based valence exchange process via the π^* orbital of the tppz bridging function. This effect is due to increasing competition from the π acceptor coligands; the efficiency of the bridge-mediated intermetallic coupling decreases with a decrease in electron density on the metal centers.

The bridging tppz ligand is a well-known redox-active center and can accommodate two electrons in the electrochemically accessible lowest unoccupied molecular orbital (LUMO).[6] The uncoordinated ancillary ligands are reduced below −1.01 V versus SCE, albeit irreversibly (Table 1). Because the complexes contain one tppz and two ancillary ligands, a total of four successive one-electron reduction waves can be expected. However, for $[\mathbf{1}]^{2+}$ and $[\mathbf{2}]^{2+}$ or **3** and $[\mathbf{4}]^{2+}$, three or two reduction waves, respectively, have been detected within the experimental potential limit (−2.0 V versus SCE) (Table 1, Figure 2). The tppz-based two reductions for the analogous dinuclear complexes having 2,2′-dipyridylamine, 2,2′-bipyridine, or 2-phenylazopyridine as ancillary ligands appeared at −0.76/−1.27, −0.60/−1.10, and −0.44/−1.43 V, respectively. Therefore, we believe that the first two reductions (couples III and IV in Figure 2 and Table 1) are essentially tppz-based processes and that the observed third reduction for complexes $[\mathbf{1}]^{2+}$ and $[\mathbf{2}]^{2+}$ corresponds to the reduction of one coligand L. The anionic nature of L^3 in **3** and the attachment of an electron-donating methyl group at L^4 in $[\mathbf{4}]^{2+}$ are factors which push the L-based reduction processes beyond the experimental potential limit.

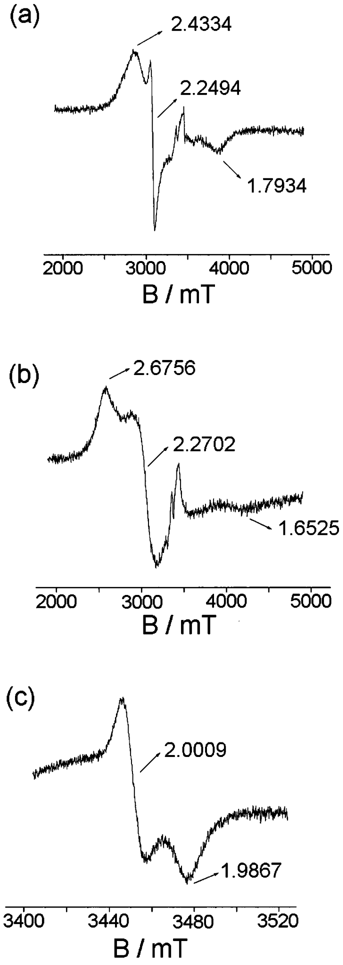

Figure 3. EPR spectra of (a) $[\mathbf{3}]^+$, (b) $[\mathbf{4}]^{3+}$, and (c) $[\mathbf{4}]^+$ in CH_3CN/0.1 M Bu_4NPF_6 at 4 K (organic paramagnetic impurities at $g \sim 2.00$ for the oxidation process).

EPR Spectroscopy of One-Electron Oxidized and Reduced Complexes. The in-situ generated oxidized species $[\mathbf{3}]^+$ and $[\mathbf{4}]^{3+}$ display rhombic EPR spectra at 4 K in CH_3CN ($g_1 = 2.433$, $g_2 = 2.249$, and $g_3 = 1.793$ for $[\mathbf{3}]^+$ and $g_1 = 2.675$, $g_2 = 2.270$, and $g_3 = 1.652$ for $[\mathbf{4}]^{3+}$) (Figure 3). Complexes $[\mathbf{1}]^{3+}$ and $[\mathbf{2}]^{3+}$ failed to show any EPR signals even at 4 K, because of rapid relaxation. The g anisotropies $g_1 - g_3 = \Delta g$ in $[\mathbf{3}]^+$ ($\Delta g = 0.640$) and $[\mathbf{4}]^{3+}$ ($\Delta g = 1.023$) are lower than the value of the Creutz−Taube ion ($g_1 = 2.799$, $g_2 = 2.489$, and $g_3 = 1.346$; $\Delta g = 1.45$[9]) despite the built-in nonplanarity of the tppz bridging ligand in the complexes. The average g factors of $\langle g \rangle = 2.175$ and 2.239 for $[\mathbf{3}]^+$ and $[\mathbf{4}]^{3+}$, respectively, are derived from $\langle g \rangle = [{}^1/_3(g_1^2 + g_2^2 + g_3^2)]^{1/2}$.[10] The distinct differences in Δg and

---

(8) (a)Hush, N. S. *Prog. Inorg. Chem.* **1967**, *8*, 391. (b) Robin, M. B.; Day, P. *Adv. Inorg. Chem. Radiochem.* **1967**, *10*, 247. (c) Hush, N. S. *Coord. Chem. Rev.* **1985**, *64*, 135.

(9) Poppe, J.; Moscherosch, M.; Kaim, W. *Inorg. Chem.* **1993**, *32*, 2640.

$\langle g \rangle$ of the one-electron oxidized dinuclear complexes can be attributed to the donor character of the ancillary ligands L′. With the weakest donors L^1 and L^2, the corresponding species $[\mathbf{1}]^{3+}$ and $[\mathbf{2}]^{3+}$ are EPR silent even at 4 K, suggesting a very large g anisotropy accompanied by strong line broadening. With the stronger neutral donor ligand L^4, the pertinent half-oxidized complex $[\mathbf{4}]^{3+}$ exhibits a detectable EPR signal with a large g anisotropy, as befits a predominantly metal-centered mixed valent species involving Ru^{III}. On changing the ancillary ligands to strongly donating anionic L^3, the corresponding semioxidized complex $[\mathbf{3}]^{+}$ displays signs of increasing ancillary ligand (L^3) participation at the singly occupied MO. The diminished contribution from the metals with their high spin−orbit coupling constants is manifested through lowered Δg and $\langle g \rangle$ values.[11] Nevertheless, the values even for $[\mathbf{3}]^{+}$ allow us to formulate these species as $Ru^{II}Ru^{III}$ mixed valent species, although the localization of spin cannot be specified with reasonable confidence in the absence of hyperfine information.[12]

In acetonitrile at 4 K, the one-electron reduced species $[\mathbf{1}]^{+}$, $[\mathbf{2}]^{+}$, and $[\mathbf{3}]^{-}$ exhibited unresolved EPR spectra corresponding to the tppz radical anion ligand with g = 2.001, 2.003, and 2.001, respectively. Complex $[\mathbf{4}]^{+}$ showed an axial EPR spectrum under those conditions with a small g anisotropy ($g_{1,2} = 2.0009$ and $g_3 = 1.9867$) (Figure 3). The isotropic g value of 1.996 is close to the free-electron value of 2.0023, which again indicates ligand-centered spin on ($tppz^{\bullet-}$), as expected.[6b,f]

UV−Vis−NIR Spectroelectrochemistry. Absorption spectra were recorded as a function of the oxidation state with the help of an optically transparent thin-layer electrolytic cell. Figures 4 and 5 illustrate the results for complexes $[\mathbf{1}]^{n}$ and $[\mathbf{3}]^{n}$, respectively, and Table 2 summarizes the wavelengths and extinction coefficients at the absorption maxima.

The spectra of the starting complexes are dominated by low-energy metal-to-ligand charge transfer (MLCT) bands from the $Ru^{II}(\mu\text{-tppz})Ru^{II}$ core. On reduction, the typical NIR bands of metal-coordinated $tppz^{\bullet-}$ ($\lambda_{max} \approx 1100$ nm) and $tppz^{2-}$ chromophores appear.[6b,f]

One-electron oxidation yields rather weak bands in the typical[1,2,6b,f,10] NIR regions for $Ru^{II} \rightarrow Ru^{III}$ intervalence charge transfer (IVCT) transitions at about 1500 nm for the trications $[\mathbf{1}]^{3+}$, $[\mathbf{2}]^{3+}$, and $[\mathbf{4}]^{3+}$. However, such a conspicuous NIR band is absent for system $[\mathbf{3}]^{+}$ containing the strongly donating anionic ancillary ligand L^3. In that case, the cyclic voltammetric and EPR results have already indicated a stronger interaction between the metals and L^3, raising the energies of Ru/L^3 mixed occupied orbitals while the acceptor LUMO (tppz) remains constant. We thus infer an IVCT transition of $[\mathbf{3}]^{+}$ at much higher energies (720 nm) than for the tricationic species. The experimental bandwidths at half-height of the IVCT features (1790, 2030, and 1530 cm^{-1} for $[\mathbf{1}]^{3+}$, $[\mathbf{2}]^{3+}$, and $[\mathbf{4}]^{3+}$, respectively) are much smaller (less than half) than the values calculated (3758, 3970, and 3854 cm^{-1} for $[\mathbf{1}]^{3+}$, $[\mathbf{2}]^{3+}$, and $[\mathbf{4}]^{3+}$, respectively) from the Hush formula.[1] In agreement with recent results for related systems,[6b,f] we take this discrepancy as an indication for class III behavior.

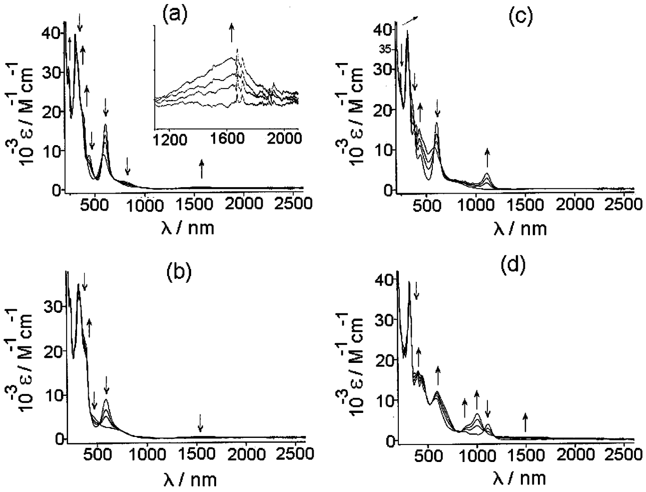

Figure 4. UV−vis−NIR spectroelectrochemistry of the conversions of (a) $[\mathbf{1}]^{2+} \rightarrow [\mathbf{1}]^{3+}$, (b) $[\mathbf{1}]^{3+} \rightarrow [\mathbf{1}]^{4+}$, (c) $[\mathbf{1}]^{2+} \rightarrow [\mathbf{1}]^{+}$, and (d) $[\mathbf{1}]^{+} \rightarrow [\mathbf{1}]$ in CH_3CN/0.1 M Bu_4NPF_6. (Inset shows the expanded part of the IVCT band.)

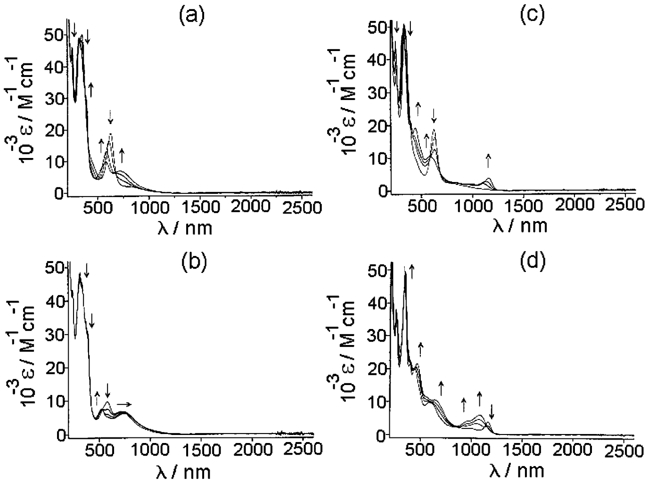

Figure 5. UV−vis−NIR spectroelectrochemistry of the conversions of (a) $[\mathbf{3}] \rightarrow [\mathbf{3}]^{+}$, (b) $[\mathbf{3}]^{+} \rightarrow [\mathbf{3}]^{2+}$, (c) $[\mathbf{3}] \rightarrow [\mathbf{3}]^{-}$, and (d) $[\mathbf{3}]^{-} \rightarrow [\mathbf{3}]^{2-}$ in CH_3CN/0.1 M Bu_4NPF_6.

On second oxidation, the L^3-containing system $[\mathbf{3}]^{2+}$ exhibits an intense long-wavelength transition at 755 nm, attributed to a mixed LMCT/LLCT transition originating from the π HOMO of L^3. In the other cases $[\mathbf{1}]^{4+}$, $[\mathbf{2}]^{4+}$, and $[\mathbf{4}]^{4+}$, the lower HOMOs result in strongly high-energy shifted transitions with $\lambda_{max} < 460$ nm.

Conclusion

Summarizing, we have shown that relatively minor modifications in structurally related ancillary ligands can have considerable consequences for the electronic structures, as evident from quite different spectroscopic properties of the mixed valent states. These results confirm in a coordi-

---

(10) Kaim, W. *Coord. Chem. Rev.* **1987**, *76*, 187.

(11) Patra, S.; Sarkar, B.; Mobin, S. M.; Kaim, W.; Lahiri, G. K. *Inorg. Chem.* **2003**, *42*, 6469.

(12) (a) Kaim, W.; Bruns, W.; Poppe, J.; Kasack, V. *J. Mol. Struct.* **1993**, *292*, 221. (b) Scheiring, T.; Kaim, W.; Olabe, J. A.; Parise, A. R.; Fiedler, J. *Inorg. Chim. Acta* **2000**, *300−302*, 125. (c) Glöckle, M.; Kaim, W.; Klein, A.; Roduner, E.; Hübner, G.; Zalis, S.; van Slageren, J.; Renz, F.; Gütlich, P. *Inorg. Chem.* **2001**, *40*, 2256.

Table 2. Electronic Spectral Data in CH_3CN/0.1 M Bu_4NPF_6 at 298 K

complex	λ_{max}, nm (ϵ/M^{-1} cm^{-1})
$[\mathbf{1}]^{4+}$	460(sh), 397(sh), 373(sh), 315(50 470), 242(sh)
$[\mathbf{1}]^{3+}$	1635(1400), 583(13 600), 390(32 480), 313(52 800), 240(38 690)
$[\mathbf{1}]^{2+}$	775(sh), 598(25 970), 442(11 140), 382(sh), 360(34 350), 306(61 700), 245(sh)
$[\mathbf{1}]^{+}$	1065(6380), 575(17 865), 425(24 560), 405(23 900), 317(57 000), 230(sh)
$[\mathbf{1}]$	1700(broad sh), 980(13 280), 855(sh), 605(19 950), 410(30 300), 313(47 980), 233(sh)
$[\mathbf{2}]^{4+}$	462(sh), 397(sh), 353(34 000), 318(sh), 256(28 000)
$[\mathbf{2}]^{3+}$	1465(440), 580(9660), 395(20 950), 350(sh), 320(32 380), 255(26 900)
$[\mathbf{2}]^{2+}$	780(sh), 605(18 480), 450(8010), 385(sh), 350(30 200), 310(40 250)
$[\mathbf{2}]^{+}$	1055(3740), 835(sh), 580(14 500), 425(15 700), 405(17 600), 320(38 400), 255(26 800)
$[\mathbf{2}]$	1710(broad sh), 990(7810), 870(sh), 617(15 900), 405(20 170), 440(sh), 330(32 700), 258(27 000)
$[\mathbf{3}]^{2+}$	755(6450), 520(7700), 392(sh), 336(sh), 310(46 400), 242(sh)
$[\mathbf{3}]^{+}$	720(7000), 578(9950), 390(sh), 337(sh), 315(48 400), 240(42 900)
$[\mathbf{3}]$	625(18 950), 347(50 400), 313(sh), 248(46 070)
$[\mathbf{3}]^{-}$	1163(3940), 583(10 700), 440(19 500), 397(21 100), 333(46 400), 255(36 900)
$[\mathbf{3}]^{2-}$	1085(6015), 950(sh), 650(10 700), 466(21 800), 343(49 500), 263(36 500)
$[\mathbf{4}]^{4+}$	460(sh), 397(21 500), 370(sh), 335(sh), 315(32 500), 275(sh), 237(31 380)
$[\mathbf{4}]^{3+}$	1555(423), 590(8970), 395(sh), 342(sh), 320(35 110), 240(31 730)
$[\mathbf{4}]^{2+}$	810(sh), 608(16 760), 442(8790), 310(40 220), 246(30 210)
$[\mathbf{4}]^{+}$	1110(4000), 584(10 600), 402(16 730), 432(15 250), 323(39 900), 260(sh)
$[\mathbf{4}]$	1450(broad sh), 1000(6560), 885(sh), 595(12 135), 405(17 330), 450(sh), 370(sh), 325(34 770)

natively defined manner the well-known sensitivity of mixed valent species toward the environment, as noted previously for changes in crystal arrangement[13] or solvation.[1,14]

Experimental Section

The precursor complex $[Cl_3Ru^{III}(\mu\text{-tppz})Ru^{III}Cl_3]$ was prepared as reported.[6e,f] 2-(2-Pyridyl)benzimidazole (L^3) was purchased from Aldrich. 2-(2-Pyridyl)benzoxazole (L^1), 2-(2-pyridyl)benzthiazole (L^2), and 1-methyl-2-(2-pyridyl)-1*H*-benzimidazole (L^4) ligands were prepared by following reported procedures.[7c,15] Other chemicals and solvents were reagent grade and used as received. For spectroscopic and electrochemical studies, HPLC-grade solvents were used. Solution electrical conductivity was checked using a Systronic conductivity bridge 305. Infrared spectra were taken on a Nicolet spectrophotometer with samples prepared as KBr pellets; far-IR spectra were recorded with samples prepared as polyethylene disks. ^1H NMR spectra were recorded for $(CD_3)_2SO$ solutions using a 300 MHz Varian FT spectrometer. UV−vis−NIR spectroelectrochemical studies were performed in MeCN/0.1 M Bu_4NPF_6 at 298 K using an optically transparent thin-layer electrode (OTTLE) cell mounted in the sample compartment of a Bruins Omega 10 spectrophotometer. Cyclic voltammetric and coulometric measurements were carried out using a PAR model 273A electrochemistry system. A platinum wire working electrode, a platinum wire auxiliary electrode, and a saturated calomel reference electrode (SCE) were used in a standard three-electrode configuration. Tetraethylammoniumperchlorate (TEAP) was the supporting electrolyte, and the solution concentration was ca. 10^{-3} M; the scan rate used was 50 mV s^{-1}. A platinum gauze working electrode was used in the coulometric experiments. All electrochemical experiments were carried out under dinitrogen atmosphere. The EPR measurements were made at 4 K with an X-band Bruker system ESP300, equipped with a Bruker ER035M gaussmeter and an HP 5350B microwave counter. The elemental analyses were carried out with a Perkin−Elmer 240C elemental analyzer. Electrospray mass spectra were recorded on a Micromass Q-ToF mass spectrometer.

Caution. Perchlorate salts of metal complexes are generally explosive. Care should be taken while handling such complexes.

Preparation of Complexes $[\{(L^1)ClRu^{II}\}_2(\mu\text{-tppz})](ClO_4)_2$, $[\mathbf{1}](ClO_4)_2$; $[\{(L^2)ClRu^{II}\}_2(\mu\text{-tppz})](ClO_4)_2$, $[\mathbf{2}](ClO_4)_2$; $[\{(L^3)ClRu^{II}\}_2(\mu\text{-tppz})]$, 3; and $[\{(L^4)ClRu^{II}\}_2(\mu\text{-tppz})](ClO_4)_2$, $[\mathbf{4}](ClO_4)_2$. All the complexes were prepared by following the same general procedure. The details are given for one representative complex, $[\mathbf{1}](ClO_4)_2$.

$[\{(L^1)ClRu^{II}\}_2(\mu\text{-tppz})](ClO_4)_2$, $[\mathbf{1}](ClO_4)_2$. The starting complex $[Cl_3Ru^{III}(\mu\text{-tppz})Ru^{III}Cl_3]$ (100 mg, 0.12 mmol) and the free ligand L^1 (61 mg, 0.31 mmol) were taken in ethanol (20 mL) and refluxed for 4 h under dinitrogen atmosphere in the presence of excess LiCl (54 mg, 1.3 mmol) and NEt_3 (0.4 mL). The initial light green solution gradually changed to bluish green. Saturated aqueous solution of $NaClO_4$ was then added to the concentrated acetonitrile solution of the product. The solid product thus obtained was filtered and washed thoroughly by cold ethanol followed by ice-cold water. The dried product was purified by using an alumina column. The dinuclear complex $[\mathbf{1}](ClO_4)_2$ was eluted by 5:2 CH_2Cl_2−CH_3CN mixtures. After removal of the solvent under reduced pressure, the product was further purified via recrystallization from a benzene−acetonitrile (1:5) mixture. Yield: 120 mg (77%). Anal. Calcd (Found) for $C_{48}H_{32}Cl_4N_{10}O_{10}Ru_2$, $[\mathbf{1}](ClO_4)_2$: C, 45.8 (46.0); H, 2.5 (2.6); N, 10.8 (11.2). Molar conductivity $[\Lambda_M\ (\Omega^{-1}\ cm^2\ M^{-1})]$ in acetonitrile: 242. IR (ClO_4^-) ν (cm^{-1}): 1085, 624.

$[\{(L^2)ClRu^{II}\}_2(\mu\text{-tppz})](ClO_4)_2$, $[\mathbf{2}](ClO_4)_2$. Yield: 112 mg (70%). Anal. Calcd (Found) for $C_{48}H_{32}Cl_4N_{10}O_8S_2Ru_2$, $[\mathbf{2}](ClO_4)_2$: C, 44.3 (44.6); H, 2.1 (2.5); N, 10.4 (10.9). Molar conductivity $[\Lambda_M\ (\Omega^{-1}\ cm^2\ M^{-1})]$ in acetonitrile: 260. IR (ClO_4^-) ν (cm^{-1}): 1082, 617.

$[\{(L^3)ClRu^{II}\}_2(\mu\text{-tppz})]$, 3. Yield: 102 mg (78%). Anal. Calcd (Found) for $C_{48}H_{32}Cl_2N_{12}Ru_2$, **3**: C, 54.5 (54.9); H, 2.7 (3.1); N, 15.5 (16.0).

$[\{(L^4)ClRu^{II}\}_2(\mu\text{-tppz})](ClO_4)_2$, $[\mathbf{4}](ClO_4)_2$. Yield: 119 mg (75%). Anal. Calcd (Found) for $C_{50}H_{38}Cl_4N_{12}O_8Ru_2$, $[\mathbf{4}](ClO_4)_2$: C, 45.8 (46.1); H, 2.7 (3.0); N, 12.5 (13.0). Molar conductivity $[\Lambda_M\ (\Omega^{-1}\ cm^2\ M^{-1})]$ in acetonitrile: 230. IR (ClO_4^-) ν (cm^{-1}): 1098, 629.

Acknowledgment. Financial support received from the council of Scientific and Industrial Research, New Delhi (India), the DAAD, the DFG, and the FCI (Germany) is gratefully acknowledged. Special acknowledgment is made to the Sophisticated Analytical Instrument Facility, Indian Institute of Technology, Bombay, for providing the NMR and far-IR facilities.

Supporting Information Available: Four electrospray mass spectra. The material is available free of charge via the Internet at http://pubs.acs.org.

IC049605C

---

(13) Webb, R. J.; Dong, T. Y.; Pierpont, C. G.; Boone, S. R.; Chadha, R. K.; Hendrickson, D. N. *J. Am. Chem. Soc.* **1991**, *113*, 4806.

(14) Glöckle, M.; Katz, N. E.; Ketterle, M.; Kaim, W. *Inorg. Chim. Acta* **2002**, *336*, 55.

(15) Addison, A. W.; Rao, T. N.; Wahlgren, C. G. *J. Heterocycl. Chem.* **1983**, *20*, 1481.